

Composition/Structure Relationships in Monolithic Borophosphosilicate Glasses Obtained by the Sol–Gel Route

C. Canevali,* R. Scotti, A. Vedda, M. Mattoni, and F. Morazzoni*

Dipartimento di Scienza dei Materiali and INSTM, Università degli Studi di Milano-Bicocca, via Cozzi 53, 20125 Milano, Italy

L. Armelao and D. Barreca

Istituto di Scienze e Tecnologie Molecolari del CNR and INSTM, Dipartimento di Chimica, Università di Padova, Via Marzolo 1, 35131 Padova, Italy

G. Bottaro

Dipartimento di Chimica and INSTM, Università di Padova, Via Loredan 4, 35131 Padova, Italy

Received August 7, 2003. Revised Manuscript Received October 24, 2003

Monolithic borophosphosilicate glasses were prepared by the sol–gel route through xerogel densification. Tetramethoxysilane ($\text{Si}(\text{OCH}_3)_4$), trimethylborate ($\text{B}(\text{OCH}_3)_3$), and trimethyl phosphite ($\text{P}(\text{OCH}_3)_3$) were used as source compounds for Si, B, and P, respectively. After drying, samples underwent thermal treatment up to 700 °C with alternating flowing oxygen and reduced pressure steps, resulting in transparent, monolithic glasses. The sample chemical composition was analyzed by X-ray photoelectron spectroscopy (XPS). Densification was investigated by vibrational spectroscopies (FT-IR, micro-Raman). The boron oxygen hole centers (BOHC) and phosphorus oxygen hole centers (POHC) paramagnetic defects generated by X-ray irradiation of glasses were studied by electron paramagnetic resonance (EPR) spectroscopy. The results obtained on borophosphosilicate glasses showed that paramagnetic defects are not created by independent processes, as expected for randomly distributed noninteracting B and P doping elements. Diamagnetic precursors of BOHC and POHC are thus proposed to be spatially close together in the glasses.

Introduction

Borophosphosilicate ternary glasses (BPSGs) have been under investigation for a long time due to their very favorable properties with respect to those of phosphosilicate (PSGs) and borosilicate (BSGs) binary glasses. Especially in the form of thin films, BPSGs are preferred to PSGs in integrated circuits, for insulating metal interconnections from the underlying polysilicon or silicide gate structures. In fact, co-doping with boron decreases the flow-temperature values (T_f) of BPSGs with respect to PSGs having the same phosphorus content.^{1,2} Such a decrease improves the gap filling and the step coverage capability of the film, allowing a more effective dielectric functionality. In addition, BPSG films are more efficient than PSGs in gettering alkali ion impurities, whose high mobility lowers the insulating properties of the glass.²

In the case of PSG and BSG layers, both thermal and insulating properties were associated with defects introduced into silica network by B and P doping elements.^{1,2} To provide a deeper knowledge of the defect structures, several authors^{3–5} performed investigations on bulk

glasses. Other studies were focused on BPSG films, either for the structure or the amount of their defects, depending on B and P content.^{6–8} Surprisingly, BPSG bulk materials were not investigated in detail even though, due to the relevant defect number expected in such samples, they should enable a more clear understanding of composition–structure relationships than films.

Due to the high interest of BPSG applications, the present work is focused on the investigation of relationships between chemical composition (B and P contents) and structural defects (type and amount) in bulk glasses. To do this, BPSG samples with different B and P contents were obtained by the sol–gel procedure in the form of monolithic, transparent regular disks (2-cm diameter). Literature reports various sol–gel synthetic approaches to bulk BPSGs: Woigner et al.⁹

* Corresponding authors.

(1) Nassau, K.; Levy, R. A.; Chadwick, D. L. *J. Electrochem. Soc.* **1985**, *132*, 409–415.

(2) Kern, W.; Schnable, G. L. *RCA Rev.* **1982**, *43*, 423–457.

(3) Griscom, D. L.; Sigel, G. H.; Ginther, J. *J. Appl. Phys.* **1976**, *47*, 960–967.

(4) Griscom, D. L.; Friebele, E. J.; Long, K. J.; Fleming, J. W. *J. Appl. Phys.* **1983**, *54*, 3743–3761.

(5) Shkrob, I. A.; Tarasov, V. F. *J. Chem. Phys.* **2000**, *112*, 10723–10732.

(6) Warren, W. L.; Shaneyfelt, M. R.; Fleetwood, D. M.; Winokur, P. S.; Montague, S. *IEEE Trans. Nucl. Sci.* **1995**, *42*, 1731–1739.

(7) Warren, W. L.; Shaneyfelt, M. R.; Fleetwood, D. M.; Winokur, P. S. *Appl. Phys. Lett.* **1995**, *67*, 995–997.

(8) Fanciulli, M.; Bonera, E.; Carollo, E.; Zanotti, L. *Microelectron. Eng.* **2001**, *55*, 65–71.

Table 1. Molar B/P/Si Glass Composition Measured by XPS

nominal composition	composition by XPS
8:0:92	5:0:95
0:8:92	0:9:91
12:4:84	7:5:88
8:8:84	8:8:84
12:8:80	9:8:83
12:0:88	8:0:92

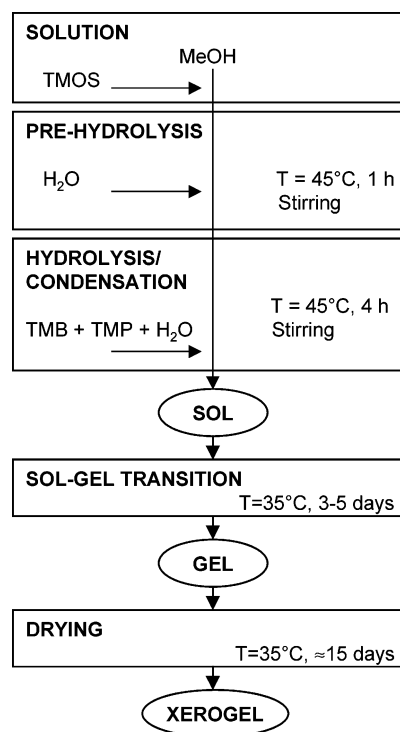
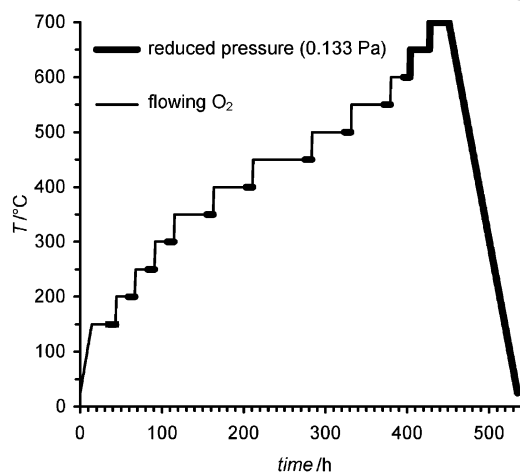
obtained crack-free glasses by densification of aerogels and Chou¹⁰ proceeded by densification of xerogels. Nevertheless, in the former case transparent glasses did not result. In the latter the amounts of B, P, and Si precursors necessary to obtain transparent glasses were not unambiguously determined. In both cases, no defect characterization was performed. Previously, the relations between B and P amounts were investigated by Kumta et al.,^{11–13} although the synthesis procedures led to powdered samples.

In this paper a procedure for xerogel densification to glass is presented that leads to transparent and crack-free bulk materials. The steps of this procedure were investigated through vibrational spectroscopies (FT-IR, micro-Raman),¹⁴ X-ray photoelectron spectroscopy (XPS) was used to determine the B/P atomic ratio in the glasses. In fact, the conventional chemical methods for element determination, which involve glass dissolution in HF, showed several drawbacks, due to the high volatility of the boron derivatives,¹⁵ and resulted in inaccurate compositional data. The content and type of defects associated with P–O and B–O linkages were studied by EPR spectroscopy, after X-ray irradiation of glasses. This treatment allowed the generation of boron oxygen hole centers (BOHC) and phosphorus–oxygen hole centers (POHC), which are EPR active probes of the diamagnetic defect precursors.^{3–8}

Experimental Section

Glass Synthesis. Glasses with B/P/Si atomic percentage ratios in the nominal range 0–12 for B and 0–8 for P (Table 1, left column) were prepared by the sol–gel method.

Si(OCH₃)₄ (TMOS, Aldrich, 98%), B(OCH₃)₃ (TMB, Strem, 98%), and P(OCH₃)₃ (TMP, Aldrich, 99+%) were used as oxide precursors. TMOS was dissolved in methanol and the solvent volume was the sum of Si, B, and P precursor volumes. Subsequently, to promote the hydrolysis of the silicon precursor, an amount of Milli-Q water (H₂O/TMOS molar ratio = 2) was added to the solution, which was then stirred at 45 °C for 1 h. Finally, TMB, TMP, and an additional 2 mol of Milli-Q water for each TMOS mole were added to the solution, under continuous stirring at 45 °C for 4 h. The resulting colorless and clear solution was kept in closed Teflon boxes at 35 °C for 4 days until gelation. Afterward, samples were aged for 2 days. Subsequently, the solvent was slowly evaporated through five small holes in the box cover. Drying of alcogels was performed for 15 days, yielding monolithic, transparent, and crack-free xerogels. The glass synthesis is summarized in Scheme 1.

Scheme 1. Flow Chart of the BSGs, PSGs, and BPSGs Sol–Gel Preparation**Scheme 2. Thermal Treatment of the Xerogels**

Densification of xerogels to glasses was carried out through thermal treatment up to 700 °C, which alternated flowing oxygen and reduced pressure steps as described in Scheme 2, to avoid inclusion of reactants in glasses.¹⁴ Transparent and monolithic glasses with density average values near those of silica glasses (value measured by conventional pycnometer: 2.00 g cm⁻³) were obtained.

The chemical composition of BPSGs, given as B/P/Si atomic ratios, was determined by XPS analysis (Table 1).

Spectroscopic Characterization. XPS analysis for B, P, and Si determination was performed on a Perkin-Elmer Φ 5600-ci spectrometer using non-monochromatized Al Kα radiation (1486.6 eV), at a working pressure lower than 5 × 10⁻⁸ Pa. The spectrometer was calibrated by assuming the binding energy (BE) of the Au 4f_{7/2} line at 83.9 eV with respect to the Fermi level. The standard deviation for the BE values was ±0.2 eV. The reported BEs were corrected for charging effects, assigning the BE value of 285.0 eV¹⁶ to the C 1s line of adventitious carbon. Survey scans were obtained in the 0–1350-eV range. Detailed scans were recorded in high-resolution mode (PE = 29.35 eV, eV/step = 0.125, dwell time

(9) Woignier, T.; Phalippou, J.; Zarzycki, J. *J. Non-Cryst. Solids* **1984**, *63*, 117–130.

(10) Chou, K. *J. Non-Cryst. Solids* **1989**, *110*, 122–124.

(11) Hsu, R.; Kumta, P. N.; Feist, T. P. *J. Mater. Sci.* **1995**, *30*, 3123–3129.

(12) Hsu, R.; Kim, J. Y.; Kumta, P. N.; Feist, T. P. *Chem. Mater.* **1996**, *8*, 107–113.

(13) Kim, J. Y.; Kumta, P. N. *J. Phys. Chem. B* **1998**, *102*, 5744–5753.

(14) Canevali, C.; Morazzoni, F.; Scotti, R.; Acierno, V.; Vedda, A.; Spinolo, G. *Mater. Res. Soc. Symp. Proc.* **2002**, *686*, A10.3.1–A10.3.6.

(15) Holleman, A. F.; Wiberg, E. *Inorganic Chemistry*; Academic Press: New York, 2001; p 970.

= 30 ms) for the O 1s, C 1s, B 1s, Si 2p, P 2s, and P 2p regions. The analysis involved Shirley-type background subtraction¹⁷ and peak area determination by integration. The atomic compositions were then evaluated using sensitivity factors supplied by Perkin-Elmer. The uncertainty on atomic compositions is ca. 10%. To evaluate the mean chemical composition of the monolithic glasses, bulk samples were preliminarily milled in a mortar and prepared as pellets. Subsequently, they were directly introduced into the XPS analytical chamber by a fast entry lock system.

Fourier transform infrared (FT-IR) spectra were recorded in the spectral range 4000–400 cm⁻¹ by a Jasco FT-IR 410 instrument. Samples were ground and mixed with dry KBr in a mortar, under a dry nitrogen atmosphere. Constant sample weight (0.003 g) and KBr amount corresponding to KBr/sample (1000 w/w) constant ratio were mixed and iso-statically pressed (41 MPa) to obtain disks. This procedure was adopted to facilitate the comparison of spectra from different samples.

Raman spectra were recorded on the monolithic samples by the micro-Raman technique, using a Dilor Labram machine excited by an Ar laser (488 nm) in backscattering configuration. The relative peak position was determined with a final accuracy of ≈ 1 cm⁻¹, referring to the emission lines from a Ne lamp. Relative peak intensities were analyzed by normalizing the spectra with respect to the SiO₂ mode at 800 cm⁻¹, which is well-separated from the other peaks, and measuring the peak intensities with respect to the baseline.

EPR spectra were recorded on monolithic glass fragments, before and immediately after irradiation with a dose of about 10³ Gy. X-ray interaction promotes the capture of electron holes (h⁺) by the structure defects associated with B and P; this generates POHC and BOHC paramagnetic defects that can be related to their diamagnetic precursors.^{3–8} Irradiation was performed at room temperature by an X-ray tube (Machlett DEG 50) operating at 30 kV. Samples were introduced into the cavity attached to a Teflon rod. The X-band CW EPR instrument was a Bruker EMX spectrometer. The EPR spectra were recorded at 123 K and the temperature control was achieved through a Bruker temperature controller for X-band spectrometer. The *g* values were measured by standardization with diphenylpicrylhydrazyl (DPPH). The relative and absolute amounts of paramagnetic species were calculated by double integration of the resonance line areas (error $\pm 5\%$) and by taking as reference the area of the Bruker weak pitch ($9.7 \times 10^{12} \pm 5\%$ spin/cm). The experimental spectra were fitted by the 6/9/91 DOS version of the SIM14S simulation program.

Results and Discussion

XPS Analysis. Conventional chemical methods for element determination that involve glass dissolution in HF suffer from the volatilization of boron fluoride.¹⁵ Concerning solid-state sampling methods, for example, Rutherford backscattering, secondary ions mass spectrometry, and X-ray fluorescence, most of them require standard glass samples. In this study, the quantification of B, P, and Si was obtained by XPS, which does not suffer from the above problems.

As a general rule, the first step in XPS spectra analysis is based on the identification of all the photoelectron lines corresponding to the different elements. Nevertheless, in a few cases some peaks arising from different species may interfere with intense signals. Specifically, one serious interference is due to the overlap of B 1s and P 2s photopeaks, which strongly occurs in oxide-based samples containing both boron and phosphorus, such as BPSGs. In fact, in these systems the above lines are characterized by very close BE

values (≈ 193 eV¹⁸). While in the case of phosphorus quantification can be made using the interference-free P 2p line, the only boron core level is 1s. As a consequence, the above overlap prevents any quantitative analysis of the B chemical state from being performed and the determination of B in BPSG systems is not straightforward. To overcome the latter problem and to evaluate both elements in the analyzed BPSG samples, the following procedure was adopted. The (P 2p)/(P 2s) area ratio equals the corresponding sensitivity factor ratio, $S(\text{P } 2p)/S(\text{P } 2s)$:

$$A(\text{P } 2p)/A(\text{P } 2s) = S(\text{P } 2p)/S(\text{P } 2s) \quad (1)$$

Since the P 2p area can be directly measured from the recorded spectra, the P 2s area can be estimated provided that the experimental $S(\text{P } 2p)/S(\text{P } 2s)$ ratio¹⁹ is known. Subsequently, the B 1s area ($A(\text{B } 1s)$) can be evaluated by the area difference of the ($A(\text{P } 2s) + A(\text{B } 1s)$) and $A(\text{P } 2s)$ signals and therefore used for computing the relative atomic percentages in all samples by the common relation¹⁶

$$C_i = 100 \frac{A_i}{S_i} \left(\sum_j \frac{A_j}{S_j} \right)^{-1} \quad (2)$$

where C_i represents the atomic percentage of the element i , while A_i and S_i stand for the area and the experimental sensitivity factor of the corresponding element peak, respectively. For silicate systems containing only B or P (BSGs and PSGs, respectively), the sample composition can be directly evaluated as B/P/Si atomic ratio.

XPS analyses were performed on ground samples. The composition values are reported in Table 1 (right column) beside the nominal compositions (left column). The P 2p peak (≈ 134 eV) was typical for P(V) in phosphates and the B 1s peak (≈ 193 eV) for B in the B₂O₃ network; the Si 2p BE (103.4 eV) pointed to the presence of a silica-based solid network.¹⁸

In the examined range of compositions, glasses retain the same P content as the sol precursors; however, B was lost up to about 40%. This behavior could be tentatively ascribed to the slow rate of both the TMOS hydrolysis and the condensation of hydrolyzed Si and B precursors.²⁰

The carbon content was below the detection limit. In the following, the experimental B/P/Si atomic ratios determined by XPS will be reported in the text.

Vibrational Investigation. The structural evolution of the samples during the densification process was studied on xerogels treated at selected temperatures, according to the heating steps in the Scheme 2. FT-IR and Raman spectra were recorded at room temperature.

As a general trend, specimens with different compositions yielded very similar results. For example, Figure 1 shows the FT-IR spectra in the range 1600–600 and

(18) Moulder, J. F.; Stickle, W. F.; Sobol, P. W.; Bonben, K. D. *Handbook of X-ray Photoelectron Spectroscopy*; Perkin-Elmer: Eden Prairie, MN, 1992.

(19) Wagner, C. D.; Davis, L. E.; Zeller, M. V.; Taylor, J. A.; Raymond, R. H.; Gale, L. H. *Surf. Interface Anal.* **1981**, 3 (5), 211–215.

(20) Irwin, A. D.; Holmgren, J. S.; Zerda, T. W.; Jones, J. J. *Non-Cryst. Solids* **1987**, 89, 191.

(16) Seah, M. P. *Practical Surface Analysis*; Briggs, D., Seah, M. P., Eds.; J. Wiley: New York, 1990; Vol. 1, p 543.

(17) Shirley, D. A. *Phys. Rev.* **1972**, 55, 4709.

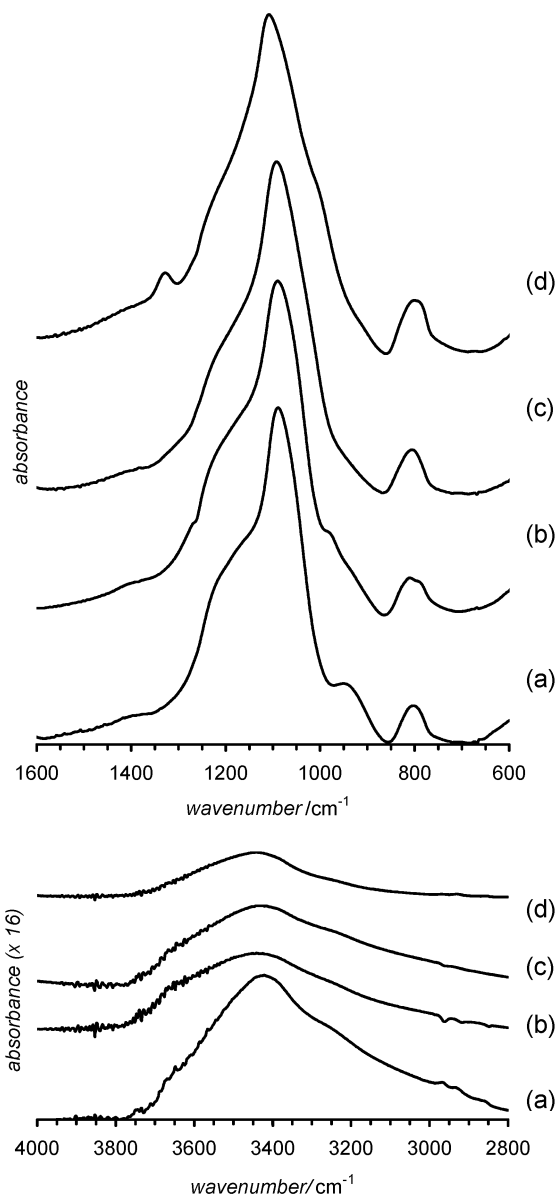
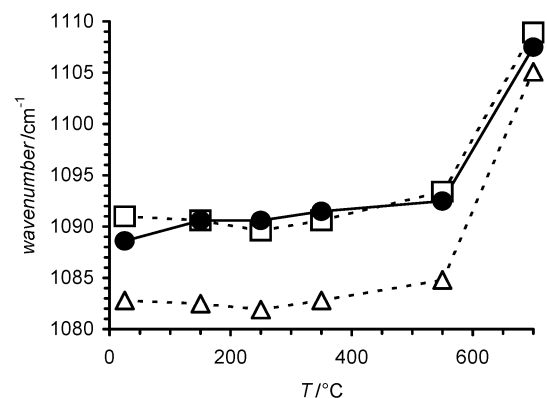


Figure 1. (bottom) FT-IR absorbance spectra in the range 4000–2800 cm^{-1} of the BPSG 8:8:84 sample (a) as prepared and treated at (b) 250 $^{\circ}\text{C}$, (c) 550 $^{\circ}\text{C}$, and (d) 700 $^{\circ}\text{C}$; (middle) the same in the range 1600–600 cm^{-1} ; (top) trend of the Si–O–Si asymmetric stretching wavenumbers vs the sintering temperature for PSG 0:9:91 (\square), BSG 8:0:92 (Δ), and BPSG 8:8:84 (\bullet) samples.

4000–2800 cm^{-1} of the B/P/Si = 8:8:84 sample both *as-prepared* and treated at increasing temperatures (250,

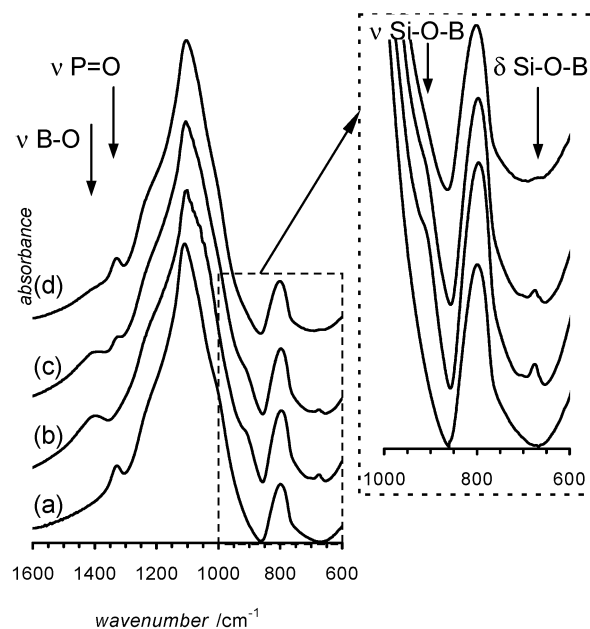


Figure 2. FT-IR absorbance spectra (1600–600 cm^{-1}) of (a) PSG 0:9:91, (b) BSG 8:0:92, (c) BPSG 7:5:88, and (d) BPSG 8:8:84 densified at 700 $^{\circ}\text{C}$.

550, and 700 $^{\circ}\text{C}$). The xerogel dehydration was assessed by the shift of the Si–OH stretching mode from 940 cm^{-1} (hydrogen-bonded Si–OH groups) in the *as-prepared* xerogel to 980 cm^{-1} (free Si–OH groups) in samples treated at 250 $^{\circ}\text{C}$. This latter vibration disappeared after treatment at 700 $^{\circ}\text{C}$.^{21,22} Dehydration at increasing temperatures was also evident from the progressive intensity decrease of the wide band at 3400 cm^{-1} due to the superimposed BO–H, PO–H, and SiO–H stretching modes²³ (Figure 1).

The glass formation was also monitored by the shift of the Si–O–Si asymmetric stretching vibration from 1089 cm^{-1} , in the xerogels, to 1104 cm^{-1} , in samples treated at 700 $^{\circ}\text{C}$. The frequency increase of this vibration was already observed during the thermal treatment of silica gels and attributed to the strengthening of the silica network in correlation with the increase of density, hardness, and refractive index.²⁴ The diagram inserted in Figure 1 reports the wavenumber shift of the Si–O–Si stretching vs the treatment temperature for 0:9:91, 8:0:92, and 8:8:84 glasses. The largest shift of this vibration occurred between 500 and 700 $^{\circ}\text{C}$ and, in agreement with previous studies on borosilicate glasses,²⁵ corresponds to the xerogel shrinkage before the glass transition temperature. At these temperatures the glass network densification occurred through structural relaxation, a bond restructuring or rearrangement process without significant weight loss.

Figure 2 reports the FT-IR spectra in the range 1600–600 cm^{-1} of glasses densified at 700 $^{\circ}\text{C}$ with composition B/P/Si = 0:9:91, 8:0:92, 7:5:88, and 8:8:84. In all the

(21) Almeida, R. M.; Guiton, T. A.; Pantano, C. G. *J. Non-Cryst. Solids* **1990**, *121*, 193–197.

(22) Bertoluzza, A.; Fagnano, C.; Morelli, M. A.; Gottardi, V.; Guglielmi, M. *J. Non-Cryst. Solids* **1982**, *48*, 117–128.

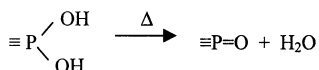
(23) Orsel, G.; Phalippou, J.; Lench, L. *J. Non-Cryst. Solids* **1986**, *88*, 114.

(24) Brinker, C. J.; Sherer, G. W. *Sol–Gel Science*; Academic Press: New York, 1990; pp 582–588.

(25) Brinker, C. J.; Sherer, G. W.; Roth, E. P. *J. Non-Cryst. Solids* **1985**, *72*, 345.

spectra, the presence of B atoms in the silica network was confirmed by the B–O asymmetric stretching mode at 1415 cm^{-1} and by the very weak peaks at 915 and 670 cm^{-1} , attributed to Si–O–B stretching and bending modes,²⁰ respectively. The Si–O–B signals, observed only in glasses treated at $700\text{ }^{\circ}\text{C}$, suggested that the inclusion of boron atoms in the silica network occurred during the heating process as observed in binary²⁰ and multicomponent borosilicates.^{13,26}

The presence of P atoms in glasses was recognized by the P=O stretching mode at 1326 cm^{-1} .²⁷ P=O peak was absent in as-prepared xerogels and appeared in glasses treated at $700\text{ }^{\circ}\text{C}$, in agreement with the following thermally activated dehydration process:



Since P=O groups are associated with defects, which are involved in the mobile charge trapping, the intensity determination of the P=O stretching vibration appears as an important step. However, more satisfactory results can be obtained considering the corresponding Raman active vibration at 1326 cm^{-1} . The diagram inserted in Figure 3 reports the intensity of the Raman band associated with the P=O vibration for PSGs and BPSGs with selected compositions. The intensity value increased with the P content and no significant difference in the band intensity, therefore in the number of P=O centers, was observed for PSGs and BPSGs with a comparable amount of P.

Figure 3 shows the Raman spectra of 0:9:91, 8:0:92, and 8:8:84 glasses densified at $700\text{ }^{\circ}\text{C}$. The main bands peaked at 440 cm^{-1} (ω_1 SiO₂ mode), 490 and 610 cm^{-1} (ν_s modes of 4-fold, D₁, and 3-fold, D₂, SiO₂ rings), 800 cm^{-1} (ω_3 SiO₂ mode), and 1060 and 1190 cm^{-1} (transverse optical, TO, and longitudinal optical, LO, ω_4 SiO₂ modes).^{28–30}

The spectra of all glasses show that the intensity ratio of both ω and D modes in Raman spectra resemble very closely those of the fully densified silica glass,^{31,32} thus confirming that the polycondensation–densification process of BPSG was already complete at $700\text{ }^{\circ}\text{C}$, a temperature lower than that necessary for pure silica sol–gel glass.

EPR Investigation. EPR investigation was aimed at identifying and quantifying the paramagnetic defects formed after X-ray irradiation of glasses. In fact, this process involves creation of electron–hole pairs which can be trapped at the defect centers.^{3–8}

EPR spectra of selected irradiated monolithic glasses, 0:9:91 (PSGs), 8:0:92 (BSGs), and 8:8:84 (BPSGs) are shown in Figure 4.

The EPR spectrum of PSG (Figure 4 line a) gave evident, though overlapped, signals of the two types of

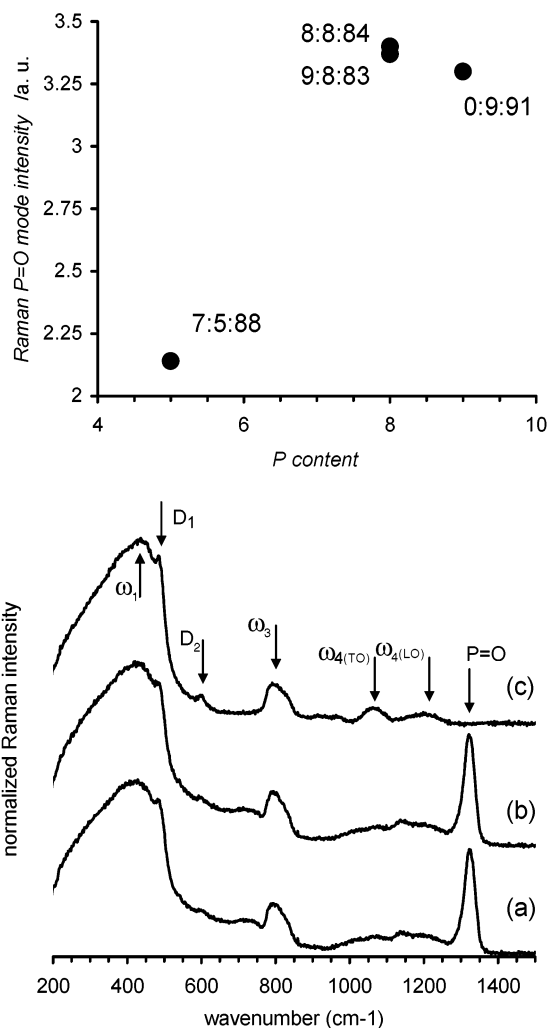


Figure 3. (bottom) Raman spectra ($1500\text{--}200\text{ cm}^{-1}$) of (a) PSG 0:9:91, (b) BPSG 8:8:84, and (c) BSG 8:0:92 densified at $700\text{ }^{\circ}\text{C}$; (top) intensity plot of the P=O stretching mode vs the P content for the glasses densified at $700\text{ }^{\circ}\text{C}$. Labels in the plot refer to the B/P/Si molar glass composition.

POHC described in the literature.^{4,6–8} POHC I, present in the major amount, was modeled as a hole shared between two oxygen atoms (both nonbridging⁴ or one bridging and the other nonbridging^{6–8}); POHC II, present as the minor component, was associated with a hole located on a single nonbridging oxygen atom.^{4,8} The total amount of POHC defects, calculated by integration of the resonance lines, was of the order of 10^{15} spin/g, a low number if compared with that of phosphorus atoms, about 10^{20} spin/g. The relative contribution of the two types of defects was not evaluated, due to the large uncertainty that could affect deconvolution of such strongly overlapped signals.

With regard to BSG, the spectrum (Figure 4 line c) showed the signals of BOHC, for which two different structures were proposed: one modeled the center as a hole trapped by bridging oxygen in the Si–O–B linkage,³ the other, more recent, suggested that the hole was trapped by a nonbridging oxygen,⁵ giving the trigonal $>\text{B}-\text{O}^{\bullet}$ center. The number of BOHC centers in BSG was of the same order of magnitude as POHC centers in PSG samples.

The presence of paramagnetic silica defects in both phosphosilicate and borosilicate irradiated glasses can-

(26) Brinker, C. J.; Haaland, D. M. *J. Am. Ceram. Soc.* **1983**, *66*, 758.

(27) Dyer, T. W. *J. Electrochem. Soc.* **1998**, *45*, 3950.

(28) Galeener, F. L. *Phys. Rev. B* **1978**, *19*, 4292.

(29) Murray, R. A.; Ching, W. Y. *Phys. Rev. B* **1989**, *39*, 1320.

(30) Sharma, S. K.; Mammone, J. F.; Nicol, M. F. *Nature* **1981**, *292*, 140.

(31) Bertoluzza, A.; Fagnano, C.; Morelli, M. A.; Guglielmi, M.; Scarinci, G.; Maliawski, N. *J. Raman Spectrosc.* **1988**, *19*, 297–300.

(32) Chiodini, N.; Meinardi, F.; Morazzoni, F.; Paleari, A.; Scotti, R.; Spinolo, G. *Solid State Commun.* **1999**, *109*, 145–150.

Table 2. EPR Data of B and P Defects in Irradiated Glasses

defect	g_1	g_2	g_3	isotope	spin	abundance %	A_1 /mT	A_2 /mT	A_3 /mT
POHC (I)	2.0082	2.0104	2.0191	^{31}P	$1/2$	100	4.688	4.890	4.625
POHC (II)	2.0036	n.d.	n.d.	^{31}P	$1/2$	100	4.417	n.d.	n.d.
BOHC	2.0035	2.0125	2.0366	^{10}B ^{11}B	3 $3/2$	19.58 80.42	1.360 0.455	1.530 0.512	0.870 0.291

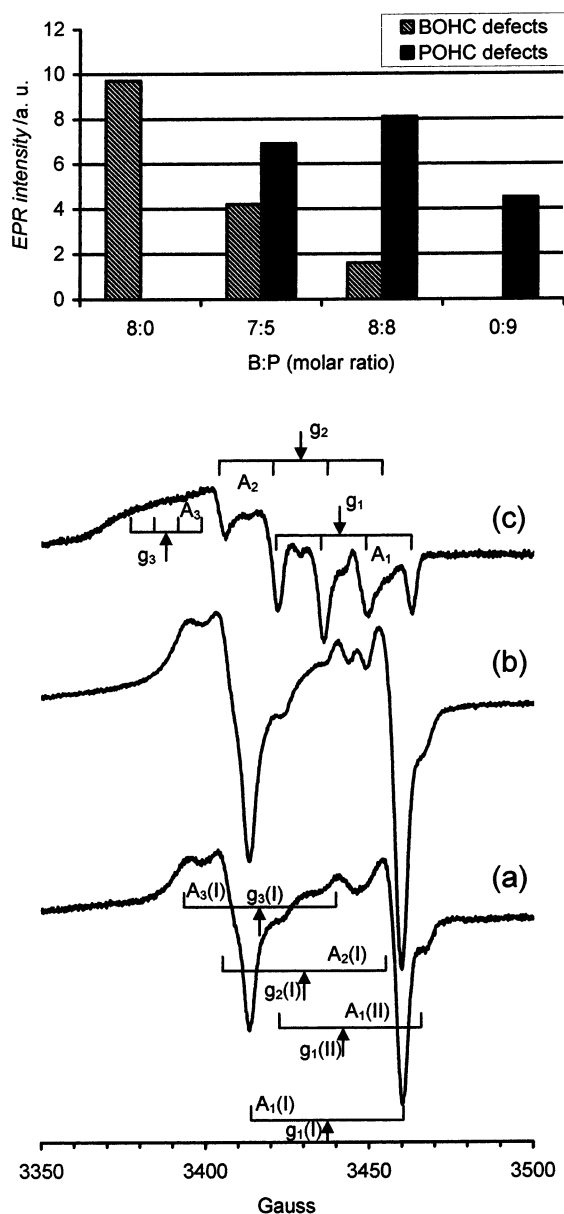


Figure 4. (bottom) EPR spectra of (a) PSG 0:9:91, (b) BPSG 8:8:84, and (c) BSG 8:0:92 densified at 700 °C; (top) histogram reporting the amount of POHC and BOHC defects, calculated by the deconvolution and fitting of the EPR spectra, for the examined glasses.

not be unambiguously ruled out because their detection in the spectra might be prevented by the higher intensity of POHC and BOHC lines.

The g and A values obtained for the recorded spectra are reported in Table 2.

As for ternary BPSGs, spectra and histograms in Figure 4 show the following:

(i) The creation of POHC is favored by the presence of boron as a co-doping element.

(ii) The BOHC amount decreases by increasing the P content.

(iii) Similarly to binary glasses, the paramagnetic defects attributable to silica were undetectable.

Accordingly it can be proposed that the competitive trapping at P–O sites is more efficient than expected from the P amount (compare the number of POHC defects in 0:9:91, 8:8:84, and 7:5:88 glasses). A spatial relation between P–O and B–O defect sites may be suggested: defects could preferentially take close location and form a hole capture section approximately equal to the sum of the capture sections of the single sites. The hole trapping by the coupled defects would be easier than for the isolated ones. Very similar behavior was observed in Ge–Sn co-doped silica glasses.³³ The diamagnetic precursor of POHC I successfully competes with that of BOHC for the hole trapping, probably because the POHC I defect shared the hole between two oxygen atoms, thus locating the unpaired electron in a more extended region with respect to BOHC.

Conclusions

The results reported in the present study concerning the preparation and the spectromagnetic characterization of borophosphosilicate monolithic glasses allow one to conclude the following:

(i) Sol–gel synthesis is suitable in preparing transparent, monolithic borophosphosilicate glasses. For the first time, XPS analysis was used to estimate the actual chemical composition of such glasses and showed that the monolithic samples retain the same P content present in the sol precursor; conversely, B was partially lost during the synthesis procedure. The residual carbon content was below the detection limit.

(ii) The number of POHC paramagnetic centers increases in ternary BPSGs with respect to binary PSGs containing the same P amount. This suggests that the defects related to B and P preferentially are closely collocated, thus trapping a greater hole number than if they were isolated. The diamagnetic precursors of POHC I have higher efficiency in hole trapping with respect to BOHC precursors.

(iii) The ability of the diamagnetic precursors of POHC and of BOHC to trap electron holes (h^+) could in principle be related to the their ability in trapping positively charged mobile ions, for example, Na^+ . The results reported in the present paper demonstrate that diamagnetic precursors of the phosphorus–oxygen hole centers may have the major role in determining the glass insulation properties and this role is enhanced in ternary BPSGs.

CM031118S

(33) Chiodini, N.; Meinardi, F.; Morazzoni, F.; Paleari, A.; Scotti, R.; Spinolo, G. *Solid State Commun.* **1999**, *112*, 565–568.